AIMS Energy, 9(2): 286–304.
DOI: 10.3934/energy.2021015
Received: 15 December 2020
Accepted: 04 February 2021
Published: 01 March 2021

http://www.aimspress.com/journal/energy

Research article

Improvement of the performance of parabolic trough solar concentrator using freeform optics and CPV/T design

Xian-long Meng*, Cun-liang Liu*, Xiao-hui Bai, De-hai Kong and Kun Du

School of Power and Energy, Northwestern Polytechnical University, 1 Dongxiang Road, Chang'an District, Xi'an Shaanxi 710072, P.R.China

* **Correspondence:** Email: mengxl@nwpu.edu.cn; liucunliang@nwpu.edu.cn.

Abstract: The developmental tendency of parabolic trough collector (PTC) is larger aperture area for energy harvest and novel optical design for higher solar concentration. Larger aperture faces a higher demand in tracking accuracy and lower tolerances with respect to wind loads, quality of mirrors, control, and mounting imprecisions. With the increase of reflection angle, the divergence size of concentrated focal spot gets enlarged on receiving surface, forming a Gaussian distribution. Receiving more energy and making best use of the concentrated solar power have become a key problem. In current study, a novel trough free-form solar concentrator (TFFC) has been developed by extending the aperture size with the aid of freeform optics and combined PV/thermal utilization. The structure model is composed by traditional parabolic trough with thermal tube, and extended freeform reflector with solar panel in slope configuration. The free-form surface is generated by geometric construction method for the sake of uniform heat flux distribution. The optical characteristics are validated by ray tracing method. The advantages will be revealed by compared with traditional system. The sensitivity analysis and error factors would be discussed as well. The initial results are promising and significant for the enhancement of trough type solar concentrator systems.

Keywords: free-form solar concentrator; PV/T; geometric construction method; ray tracing method; heat flux distribution

1. Introduction

Solar energy as one of the most promising renewable energy resource, is capable of providing

both electrical and thermal power. Concentrated solar power (CSP) enables the collection of a large amount of solar rays onto small area for heat transfer or electricity generation. Solar concentrator is the key component for energy collection that including point focusing and line focusing types [1]. Compared with point focusing type, line focusing concentrators such as parabolic trough collector (PTC) occupies more installed capacity in the world [2,3], which although provides lower solar concentration ratio, but can be simpler to manufacture and higher cost-performance ratio [4]. In order to reduce the cost of electricity and gain competitiveness, there are two developmental tendencies for PTC: (i) designing novel optical system for higher solar concentration that close to the ideal concentration. (ii) developing larger aperture area for energy harvest which implies a higher demand in tracking accuracy and lower tolerances with respect to wind loads, quality of mirrors, control, and mounting imprecisions. For instance, current state-of-the-art PTC-SpaceTube collector has a very large aperture of 8.2 m × 16 m and rim angle of 82 deg [5]. The drawback of increased aperture size lies in larger error factor and optical loss. In such case the structural behaviors under gravity and wind loading faces big challenge that will dramatically reduce the optical performance [6]. The optical errors of solar concentrating system decrease over time because of dust and aging phenomenon of solar tracking system and reflecting mirrors. With the increase of reflection angle, the divergence size of concentrated focal spot gets enlarged on receiving surface, forming a Gaussian distribution. Energy at higher grades is obtained by the receiving center, whereas energy with lower concentration appears at edge region. How to receive more energy and make best use of the concentrated solar power have become a key problem.

With the fast development of advanced machining technologies, freeform optics has been introduced to CSP area in recent years. Freeform surface does not have a fixed mathematical expression which is constructed by several curved surfaces such as B-spline patches [7]. This technology therefore achieves much higher design freedom which can be applied for precise control of energy transmission. Freeform optics has become a hot topic especially in the area of illumination engineering [8], imaging optics [9]/non-imaging optics [10] and solar energy [11]. Concentrating Photovoltaics is the major field that widely adopts freeform optics in order to improve the efficiency, compactness and error tolerance [12]. One representative work lies in the XR type Concentrated Photovoltaics (CPV) modules used in off-axis structure [11,13,14]. The optical system, composed by primary 'X' reflector and secondary 'R' lens, was designed by SMS method [15]. The tested output efficiency of assembled module reaches 33% with the solar concentration of 1000x. Other CPV modules based on similar Köhler lighting principle have been developed by the same group [16–18], including Fresnel-lens-based FK module [19,20], TIR-R modules [21] and Cassegrain RXI modules [16] that achieves different characteristics. However, few studies above focused on hybrid PV/T applications and PTC system.

The generation of freeform surface is the key technology that affects the surface error and feasibility of production. Because of the complexity, there is no universal method for all kinds of engineering problems. Available methods include multi-parameter optimization [22], Wassermann-Wolf differential equation method [23], tailoring method [24], point-to-point mapping [25], simultaneous multiple surface method (SMS) [26] and Geometric Construction Method-GCM [27]. GCM is a direct method that generates the reflecting/refracting mirror of optical system using every single ray as a bridge. It is especially suited for the problem when a specific relation between light source and target is required.

The current study aims to achieve higher receiving energy as well as optical efficiency by

extending the aperture size of PTC using freeform optics and combined PV/thermal utilization. To make the best use of concentrated Gaussian distribution, the new structure model is composed by traditional parabolic trough with thermal tube, and extended freeform reflector with solar panel in slope configuration. The free-form surface is generated by GCM for the sake of uniform heat flux distribution. The optical characteristics are validated by ray tracing method. The advantages will be revealed by compared with traditional system. The sensitivity analysis and error factors would be discussed as well. The simulation results are promising and significant for the enhancement of trough type solar concentrating systems.

2. Optical modelling

In order to clearly explain the design intention of TFFC, geometrical optics principle of parabolic reflectors would be simply introduced here. As is known, smaller focal spot size as well as higher concentration ratio are key factors for solar concentrating system. Here we define the error factor θ as a comprehensive parameter that levels tracking accuracy and mirrors, control and mounting imprecisions, slope errors, and sun shape. Thus the width of focal spot (perpendicular to reflecting vectors) depends on the structural parameter of parabolic concentrator, as the following equation tells:

$$W = \frac{4f \cdot \tan\theta}{1+\cos\psi} \tag{1}$$

where f represents the focal length. ψ is the angle that a straight line going from any point on PTC to the focus makes with the optical axis, ranging between 0° ~ 90°.

It can be seen in Figure 1 that the divergence size W apparently increases with included angle ψ. Here the focal length f and error factor θ are 2.358 m and 14 mrad. Traditional imaging concentrator, such as parabolic dish/trough concentrators present a Gaussian distribution at receiving surface. With the increased distance by the optical axis, the concentrated heat flux decreases dramatically. Energy at higher grades is obtained by the receiving center, whereas energy with lower concentration appears at edge region. In another words, the solar rays collected at the outer part of parabola is more suitable for PV conversion.

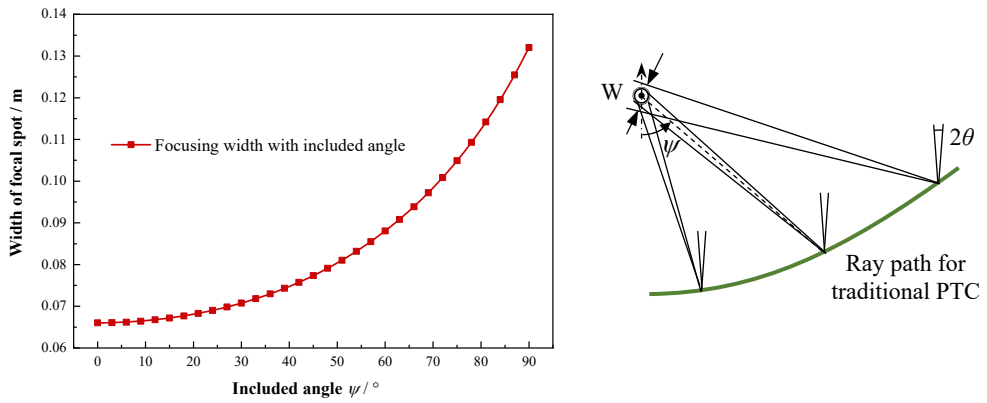

Figure 1. Width of focal spot formed by imaging solar concentrator.

The distribution law of focal spot, to a great extent, determines the choices of receiver size. The effect of error factor and tube receiver size on the intercept ratio of PTC have been revealed in Figure 2. The size of solar thermal tube is normally limited for the purpose of lower heat loss. Therefore the radius of tube for PTC is generally less than 45 mm. We can find the intercept ratio gradually declines along with the increase of error factor, when more rays were reflected outside to be lost. Compare different size of thermal tube between 20–45 mm, larger thermal tube gets apparent improvement on intercept ratio, and the optical loss at high error factor become less obvious. When the radius of thermal tube is 20 mm, the intercept ratio is lower than 0.75 even for the case of 11 mrad error factor. For the tube of 45 mm, it reaches close to 1.0 especially for the error factor smaller than 14 mrad. Under actual condition, the optical errors of solar concentrating system decrease over time because of dust and aging phenomenon of solar tracking system and reflecting mirrors. How to increase the optical efficiency for the limited size of thermal tube is therefore a necessity.

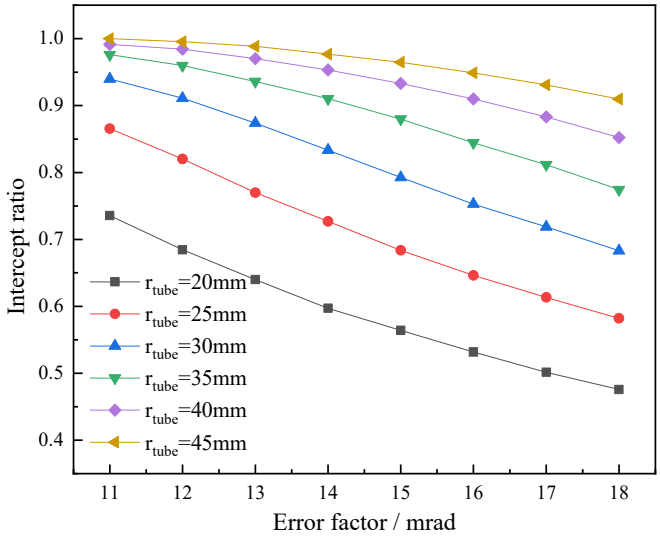

Figure 2. Effect of error factor and tube receiver size on the intercept ratio of PTC.

The developmental tendency of PTC in future is larger aperture area that ensures sufficient receiving energy but meanwhile implies higher demand in tracking accuracy and lower tolerances with respect to wind loads, quality of mirrors, control, and mounting imprecisions [6]. The current study aims to achieve higher receiving power & optical efficiency by extending the aperture size using freeform optics and combined PV/thermal utilization. To make best use of collecting solar power, a thermal tube absorber (assume to be narrower than local focal size) is arranged just at the focus to collect the receiving energy from parabolic region, where the width of focal spot tends to be smaller so the optical loss is limited, as Figure 2 shows. This part ensures maximum concentration ratio by using highly commercialized and developed PTC module. A pair of symmetrical PV panels is then put on the top of tube receiver with the edge ray cutting the bottom (starting point $\mathbf{S_{pv}}$) to totally stagger the reflected rays by parabolic region and avoid local overheating. The objective of freeform reflector is to form uniform irradiance as well as higher efficiency for solar panel. Two symmetrical PV panels with a certain slope angle were employed instead of parallel panels (parallel with xoy surface) to decrease the optical loss from the back of PV panels, allowing more solar rays reaching the reflecting surface. The accuracy restriction for the outside surface structure can be

relaxed based on CPV application.

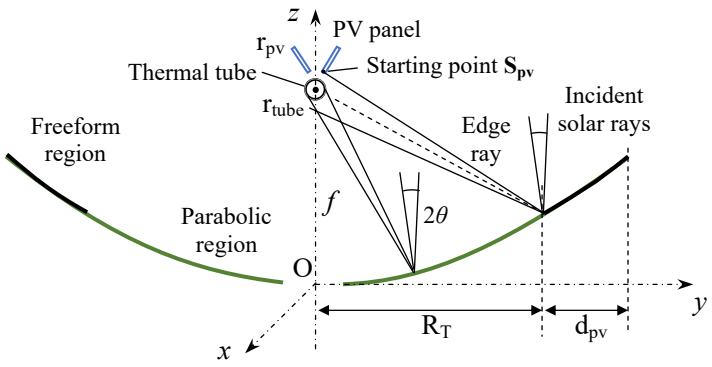

Figure 3. Sketch of the TFFC structure and rim ray tracing.

The structural parameters in Figure 3 for optical simulations are as follows: the optical axis of primary PTC is set as the z-axis in Cartesian coordinate. The parabola origin coincides with coordinate origin O. And all the optical/receiving components of TFFC have the length of 1000 mm along x-axis. The radius of parabolic reflector is defined as R_T and the length of freeform region is set to be d_{pv}. The tube absorber is arranged on the focal point in length *f*. In addition, to support the receiver located along the focal line of the parabola, a small gap (Gap) between two halves of the reflector are given to install the flange or support the bracket. It also reduces the cost of the reflector manufacture without losing efficiency, since the receiver always shadows this area. In order to avoid overheating by the parabolic reflector, a pair of symmetrical PV panels is put on the top of tube receiver based on the starting point $\mathbf{S_{pv}}$ which just passed through the outside edge ray reflected from parabolic region. The length of PV panel is r_{pv} that is highly relative with CPV concentration ratio. The slope angle needs to be calculated for the maximum optical absorption in lowest incident angle. That is, the normal at the center of PV panel coincide with the bisector of freeform reflector.

3. Freeform surface generation & Mathematical model

In order to effectively utilize the outer edge region of Gaussian heat flux, the reflector in freeform region is constructed based on 2D-geometric construction method (GCM). GCM is a direct method that generates the reflecting/refracting mirror of optical system using every single ray as a bridge. It is especially suited for the problem when a specific relation between light source and target is required. Based on the principle of GCM, Y Cheng (2012) joined continuous small planar surface to construct the free form mirrors, which is applied in the non-imaging illumination system [28]. This traditional method using planar surface has the disadvantage of high surface error. To solve this problem, curve segments have been considered as an improvement. C Tsai developed a free-form concentrator for the improvement of heat flux uniformity on solar cell [27] using the method of connecting several circular arc segments together to form a profile. In the current study, a similar model is developed for trough solar concentrator with PV/Thermal hybrid application, called Curved Geometry Construction Method (CGCM). The points generation procedure is shown in Figure 4. The following steps had been adopted:

1) Assume the initial point $\mathbf{P}_{s,0}$ emits one ray/vector (expressed as $\mathbf{v}_{s,0}$) and intersects with target

curved surface at point $\mathbf{P}_0$ which locates at the outer boundary of parabolic trough. According to the target point $\mathbf{P}_{t,0}$ (or $\mathbf{S_{pv}}$ as the starting point) and vector $\mathbf{v}_{t,0}$, the local normal vector is solved as $\mathbf{n}_0 = \frac{\mathbf{v}_{t,0}}{|\mathrm{V}_{t,0}|} - \frac{\mathbf{v}_{s,0}}{|\mathrm{V}_{s,0}|}$, and the extended line segment of normal vector can be expressed as $\overline{\mathbf{C}_0\mathbf{P}_0} = \mathbf{P}_0 + \lambda_0 t_0$, where t_0 represents the argument.

2) The second point $\mathbf{P}_{s,1}$ emits a parallel ray at the vector of $\mathbf{v}_{s,1}$ that will be reflected by the curved surface and hit the target point $\mathbf{P}_{t,1}$. There exists a scalar value $\lambda_{s,1}$ that make the solar ray $[\mathbf{P}_{s,1}, \mathbf{v}_{s,1}]^T$ intersect the surface at point $\mathbf{P}_1$:

$$\mathbf{P}_1 = \mathbf{P}_{s,1} + \lambda_{s,1}\mathbf{v}_{s,1} \tag{2}$$

Until now, the position of $\mathbf{P}_1$ can be obtained if the value of $\lambda_{s,1}$ is known.

3) To solve the scalar value of $\lambda_{s,1}$, we can assume that the elementary arc segment $\overset{\frown}{\mathbf{P}_0\mathbf{P}_1}$ presents a circular curve. According that the normal vector $\mathbf{n}_0$ and $\mathbf{n}_1$ are both vertical to the freeform profile, the relationship as follows can therefore exists:

$$\overline{\mathbf{C}_0\mathbf{P}_0} = \overline{\mathbf{C}_0\mathbf{P}_1} \tag{3}$$

In this formula, $\mathbf{P}_0$ is a known value, and $\mathbf{P}_1$ can be solved using this equation:

$$\mathbf{P}_1 = \mathbf{P}_{s,1} + \lambda_{s,1}\mathbf{v}_{s,1} \tag{4}$$

where C_0 is the intersection between vector $\mathbf{n}_0$ and $\mathbf{n}_1$. The line segment $\overline{\mathbf{C}_0\mathbf{P}_0}$ is the single function of argument t_0 and can be obtained using:

$$\overline{\mathbf{C}_0\mathbf{P}_0} = \mathbf{P}_0 + \mathbf{n}_0 t_0 \tag{5}$$

In the same way, $\overline{\mathbf{C}_0\mathbf{P}_1}$ can be expressed as:

$$\overline{\mathbf{C}_0\mathbf{P}_1} = \mathbf{P}_1 + \mathbf{n}_1 t_1 \tag{6}$$

where $\mathbf{P}_1$ can be known by Eq (3). $\mathbf{n}_1$ represents the local normal vector and can be calculated by:

$$\mathbf{n}_1 = \mathbf{Rot}(y, \theta_1)(-\mathbf{v}_{s,1}) \tag{7}$$

where $\mathbf{v}_{s,0}$ is the known emitting vector, θ_1 is the equally divided angle of incident and reflected angle:

$$\theta_1 = \frac{1}{2}\cos^{-1}(-\mathbf{v}_{s,1} \cdot \mathbf{v}_{t,1}) \tag{8}$$

Once the scalar $\lambda_{s,1}$ is solved, coordinate $\mathbf{P}_1$ and corresponding normal vector $\mathbf{n}_1$ can be obtained by Eqs (4) and (7). In the same manner, points $\mathbf{P}_2$, $\mathbf{P}_3$, $\mathbf{P}_4$ and local normal vectors can be solved. The freeform profile can be generated by connecting these discrete points. Note that the incident vector $\mathbf{v}_{s,0}$ and $\mathbf{v}_{s,1}$ are equally parallel with incident solar rays. The sampled target points on PV panel $\mathbf{P}_{t,0}$,

$\mathbf{P}_{t,1}$, etc. should be evenly distributed along a certain radius depending on the preset solar concentration.

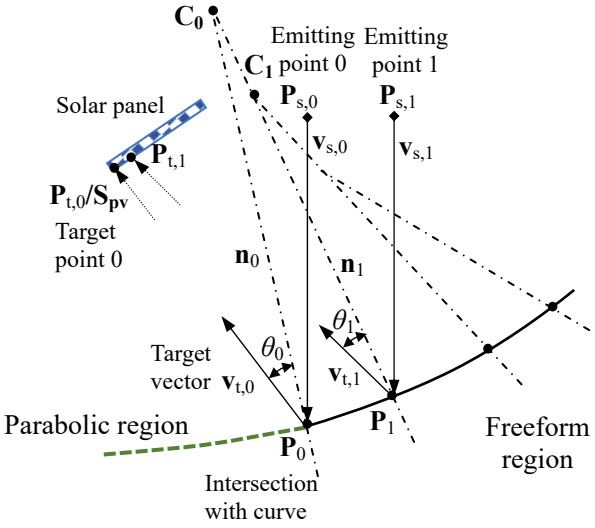

Figure 4. Generating freeform curve of TFFC using CGCM.

Table 1. Structural parameters of TFFC for ray-tracing simulations.

Parabolic surface	Freeform surface	Solar thermal tube	PV receiver
Focal length = 2358 mm, Aperture = 4100 mm, Length along x-axis = 1000 mm, Gap distance = 400 mm, Reflectivity = 1.0	CG = 5.0x, Length d_{pv} = 1741.7 mm, Number of discrete points = 50, Length along x-axis = 1000 mm Reflectivity = 1.0	Diameter = 70 mm, Thermal energy ratio = 0.7, Length along x-axis = 1000 mm, Absorptivity = 1.0	Coordinates Y of $\mathbf{S}_{pv}$ 50 mm, Width r_{pv} = 234 mm, Slope angle α = 72.85°, PV energy ratio = 0.3, Length along x-axis = 1000 mm, Absorptivity = 1.0

It is certain that as the points number increase, the generated curve becomes more accurate. The current model selected 50 points to create the B spline curve as well as the trough surface with the aid of CAD software. The data of calculated points are presented in the Appendix A. Ray tracing technology is adopted to investigate the energy transmission performance of TFFC, which are based on the typical structural parameters in Table 1. The number of sampled solar rays was 10^8 ensuring the simulation accuracy. Also the half angle of acceptance was fixed to 14 mrad as a realistic value for tracking accuracy, quality of reflecting mirrors, and control and mounting imprecisions for the order of magnitude of the aperture range. In addition, it should be noted that all the surface and absorber components are treated as ideal surface with the reflectivity/absorptivity value of 1.0.

4. Simulation results and discussion

The following sections discuss the optical simulation results of TFFC. The advantages will be revealed by compared with traditional system. The sensitivity analysis and error factors would be discussed as well.

4.1. Improvements by the new optical system

4.1.1. Ray path and model verification

Straightforward expressions of the optical transmission characteristic of the novel design are presented using the paragraphs of sampled ray path, as Figure 5 shows. In ideal condition, concentrated solar rays are all collected by the thermal tube when the error factor is zero and solar concentration reaches a maximum. In actual conditions, however, the reflecting vectors present a certain randomness caused by the tracking error, reflecting error, etc. The ray path in Figure 5(c) presents the ray path of parabolic trough with error factor of 14 mrad. We can find a portion of solar rays reach the thermal tube with some others lost because of the limited size of tube.

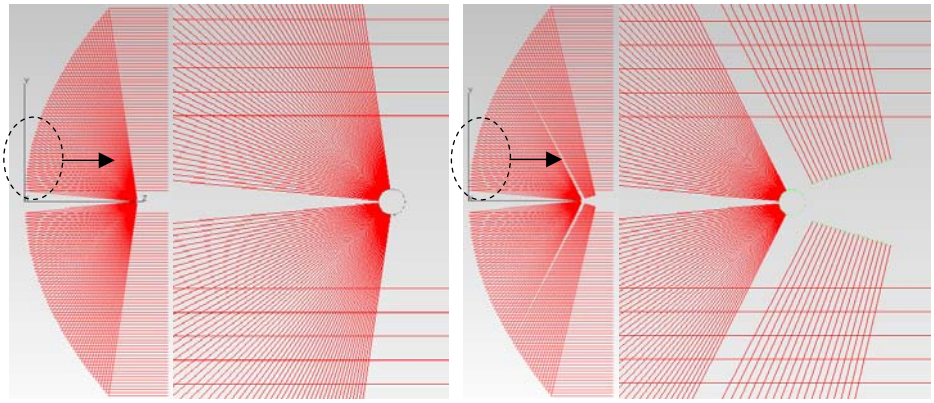

(a) Traditional parabolic trough (b) TFFC

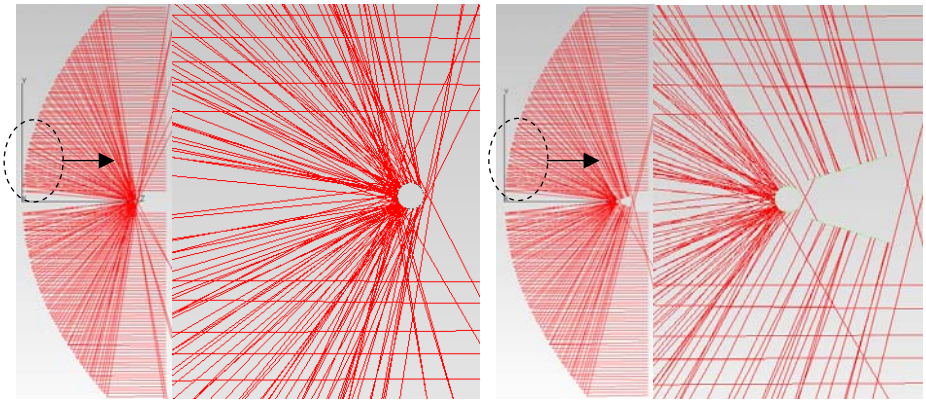

(c) Traditional parabolic trough with error factor (d) TFFC with error factor

Figure 5. Comparison of the ray path between parabolic trough and TFFC.

Compared with the original PTC, the new proposed TFFC adopts freeform reflector compared with PV panel to collect the edge part of Gaussian heat flux. As can be seen in Figure 5(b) and (d), the concentrated solar rays are divided into two parts by TFFC: some are collected by the thermal tube at center, while the rest are reflected to the PV receiver outside. Without error factor, the optical

efficiency/intercept factor reaches 1. The solar rays collected by the freeform reflector distributes evenly on the solar panel and forms a uniform irradiance. A 'blank area' exists between PV and thermal absorber where no rays pass through. The simulation result has totally met our expectance by freeform optics that will verify our proposed model. For the case with error factor (Figure 5(d)), on the other hand, optical loss also exists. Some rays passed through the 'blank area'. Also note that the rays still spread uniformly on the solar panel. This would be proved again in the following parts.

4.1.2. Improvements at different error factor

Since several factors including error factor, aperture size and PV ratio will influence the intercept ratio, as Figure 6 shows. Here PV ratio = 0 means traditional PTC system was adopted for totally thermal use (Figure 6(a)). We can find that the intercept ratio drops dramatically with the increase of error factor as well as aperture size. For the case of 18 mrad error factor and 10 m aperture, the intercept ratio dropped to 0.68. This can be easily explained by optical loss through outer edge of reflector.

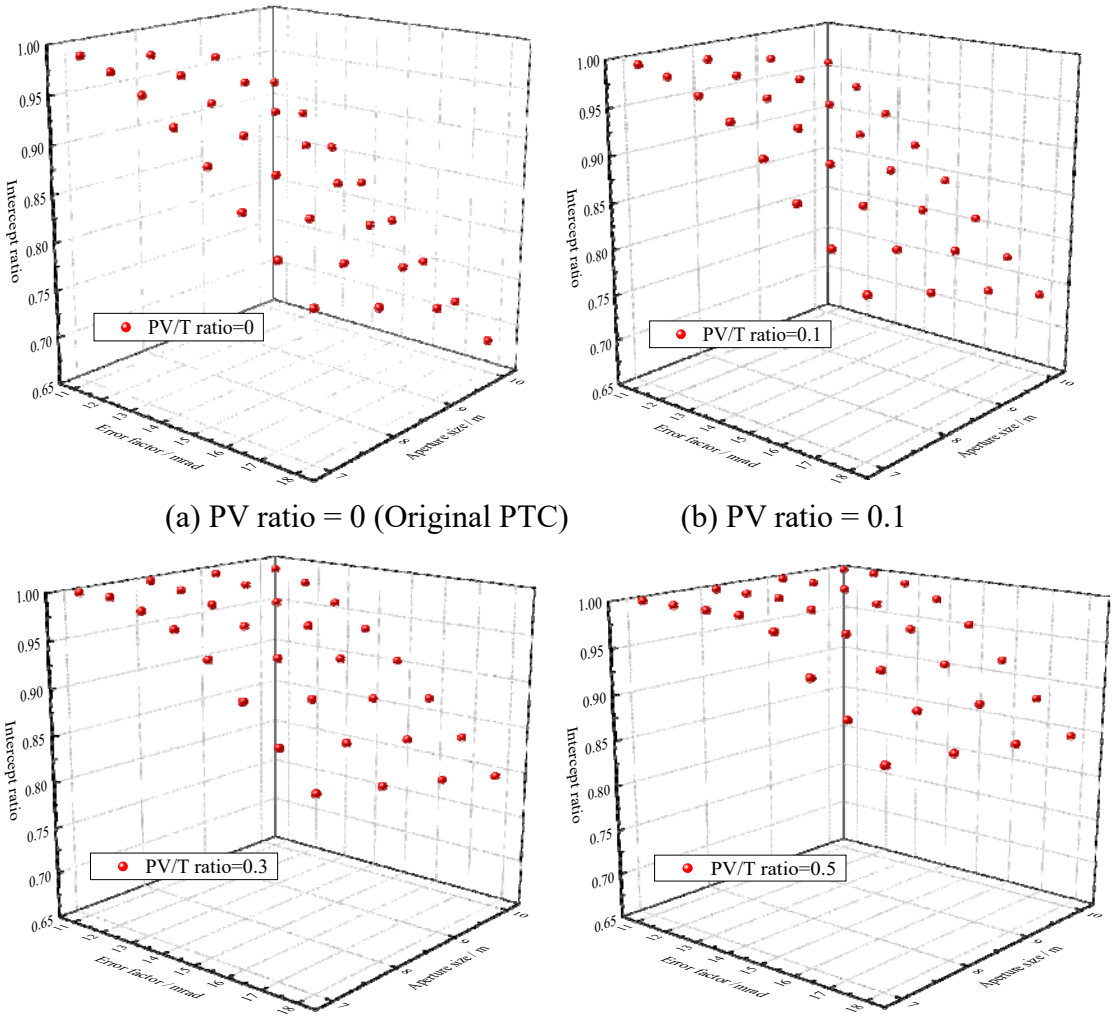

(a) PV ratio = 0 (Original PTC) (b) PV ratio = 0.1

(c) PV ratio = 0.3 (d) PV ratio = 0.5

Figure 6. Comparative study between novel design and traditional system.

In order to recuperate the energy in an efficient way, the edge part of solar rays were collected by freeform surface for electricity generation with PV ratio between 0.1–0.5. It can be found in Figure 6(b)–(d) that the new design system has improved the optical efficiency remarkably. With the aid of TFFC, the effect of aperture size on intercept ratio has been slowed down. We can see that the intercept ratio changed slightly when PV ratio equals to 0.3 and 0.5. The error factor still makes important impact. Obvious decrease can be observed when the error factor is larger than 14 mrad. For PV ratio = 0.5, the intercept ratio at in the worst case had been improved to 0.85 which corresponds 0.68 for traditional PTC. The optical loss is totally caused by the part of central parabolic region for thermal receiver. In addition, it should be note that at smaller error factor within 14 mrad, the intercept ratio for case PV ration = 0.5 tends to be stable at 1.0.

The effect of aperture size and error factor for original PTC and TFFC system with PV ratio of 0.3 have been revealed in Figure 7. We can find the intercept ratio, ranging between 0.7 and 1.0, decrease dramatically with larger aperture size and error factor because of apparent optical loss. Especially for the case of 10 m aperture and 18 mrad error factor, the intercept ratio reaches as low as 0.727. By compared, with the aid of new designed TFFC system the optical performance was remarkably improved. The intercept ratio for 0.3 PV ratio reaches 0.806. At large aperture size such as 9 m and 10 m, the intercept ratio of TFFC system keeps higher than original PTC at different error factors. For the case of 7 m and 8 m aperture, on the other hand, TFFC system has little effect at low error factor. 7 m aperture with 11 mrad–13 mrad error factor, for instance, obtains lower intercept ratio than original PTC system. At higher error factor the situations get better obviously. Above phenomenon tells that TFFC is suitable for large aperture size and error factor.

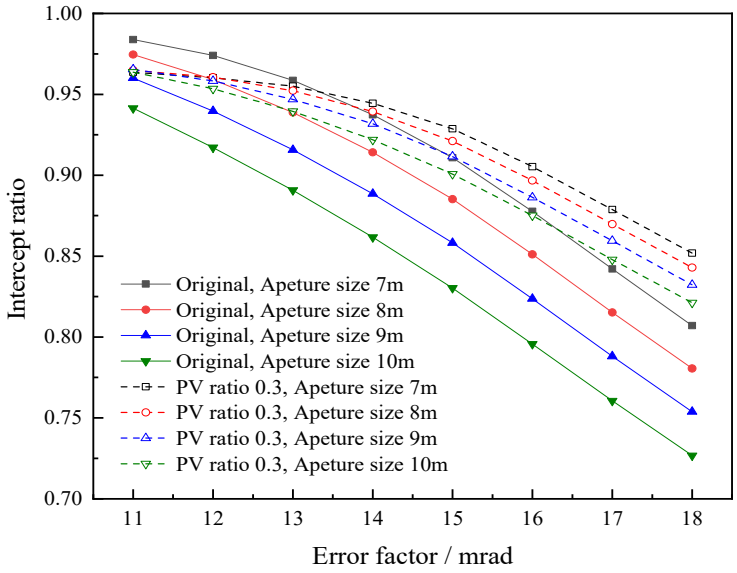

Figure 7. Effect of error factor and aperture size for original PTC and TFFC.

4.2. Sensitivity analysis of TFFC

4.2.1. Effect of PV Geometric Concentration Ratio

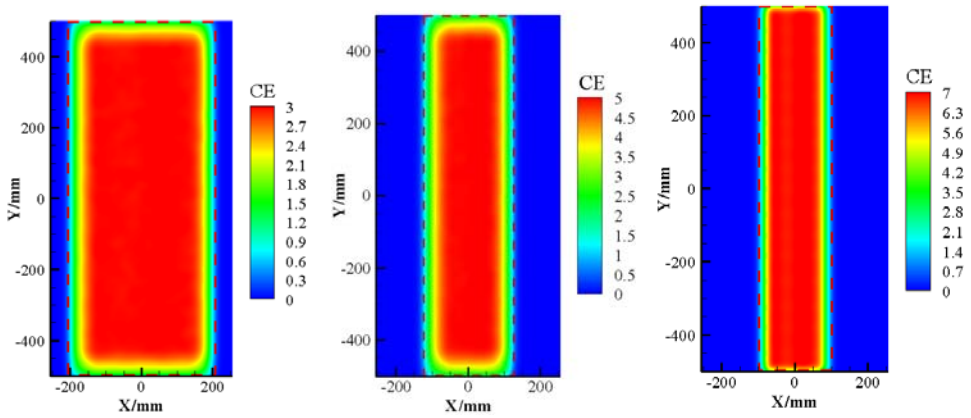

(a) CG = 3.0 (b) CG = 5.0 (c) CG = 7.0

Figure 8. 2-D Irradiance distributions on solar panel with different PV concentration.

Geometric Concentration Ratio (CG) is defined by the ratio of input/reflecting area to output/receiving area, which has a dominant effect to the heat flux distribution on solar receiver. This effect has been presented in Figure 8 using 2-D distribution and Figure 9 using section distribution with CG between 3–7 suns. The red dashed squares are the area of solar panel. The value of division CE is a dimension of receiving solar radiation using heat flux divided by 1000 W/m^2 (One sun energy density). We can find the concentrated heat flux remains high uniformity and coincide with the preset CG. Along with the increase of preset CG value, the receiving area covered on PVR become apparently smaller and the uniformity becomes worse. A sharp decrease appears at the edge part of receiver that was caused by the divergence angle of reflecting ray vectors.

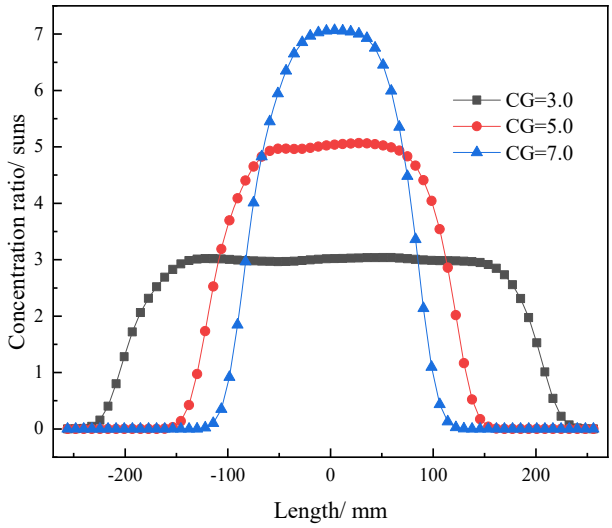

Figure 9. Concentration distributions on solar panel along y = 0 section under different C_G.

4.2.2. Effect of PV/T ratio

The energy allocation for PV/Thermal use makes great impact on optical performance of TFFC. Here we define 'PV ratio' as the occupation of PV energy to the total energy. The optical characteristics with PV ratio of 0.1, 0.2, 0.4 were investigated, as Figure 10 shows. Since the simulation premise is the same preset C_G, we can find that the irradiance uniformity declines as the PV ratio is low. Especially in the case of PV ratio = 0.1, the dropping trend of heat flux at the edge had become more obvious that will influence PV energy conversion. This was caused by the limited area of freeform reflector that makes the error factors lead the optical transmission. On the contrary, the uniformity of irradiance distribution was much improved with the increase of PV ratio. Above phenomenon tells us that a reasonable CG is necessary in practical application when low a PV ratio was selected.

The accuracy restriction for the outside freeform surface structure can be relaxed based on CPV application. Figure 11 presents the heat flux distributions considering different error factors of 10 mrad, 14 mrad and 18 mrad. According to the simulation, the main central part of solar panel remains the solar concentration of 5.0 suns. With the increase of error factor, however, the energy distributes on slightly smaller area which makes the receiving energy lower. The degree of impact is not high that only the edge region of receiver drops, causing energy deficiency. This is an inspiring result for the control of optical loss when we replace a part of freeform surface to the original PTC.

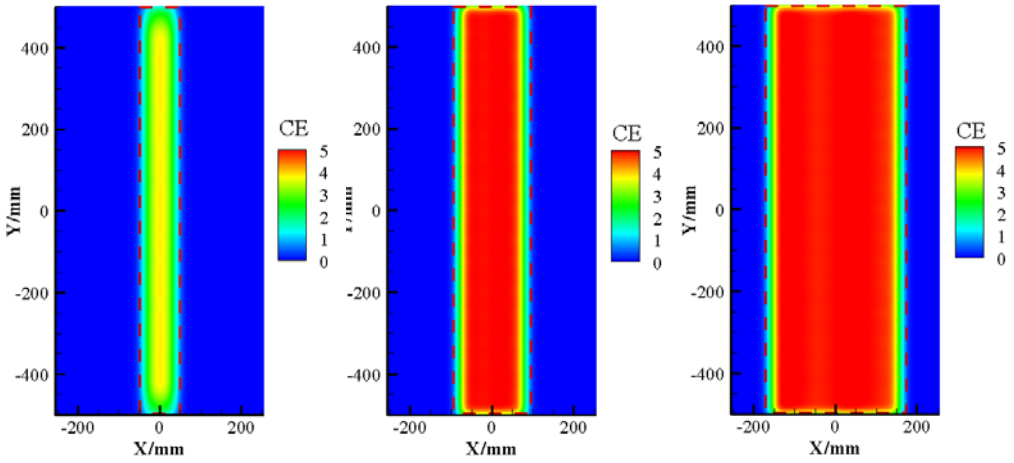

(a) PV ratio = 0.1 (b) PV ratio = 0.2 (c) PV ratio = 0.4

Figure 10. 2-D Irradiance distributions on solar panel with different PV ratio.

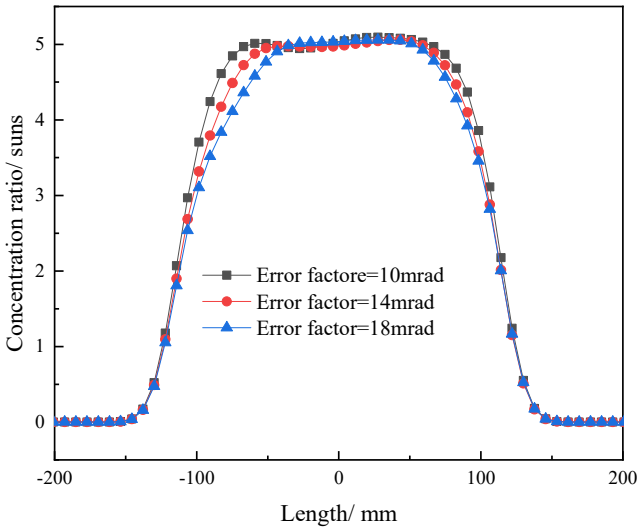

Figure 11. Concentration distributions under different error factors.

4.2.3. Effect of tracking angles

Solar tracking error will cause the mismatching problem and seriously influence the optical transmission, output efficiency and life expectancy of receiving modules. Therefore the effect of angle transmission is necessary to be studied. Performance of tracking angle rotated in x-axis is the main focus for solar trough concentrating system, as Figure 12 shows. Optical efficiencies of new designed TFFC, LS3/Eurotrough and two stage PmTC [6] have been compared. The LS3 and PmTC are using the same size of thermal tube as current study (same tube radius in 35 mm). Error factor of LS3 and PmTC are 12 mrad and 14 mrad. And the corresponding aperture widths are 5.76 m and 8.12 m, respectively. We can see that the intercept ratios of LS3 and PmTC stabilize at 1.0 in low tracking angle but drops dramatically around 12 ~ 20 mrad. Optical efficiency of new TFFC, on the other hand, decreases gradually within 20 mrad angle and generally keeps lower than the other two concentrators. It can be obviously found that the angle tolerance of TFFC is much better than PTC. The thermal receiver combined with PV panels keeps receiving solar radiation within 110 mrad angle. Two crests of receiving power appears at 0 mrad and 40 mrad, respectively. Improvements at second point (40 mrad) is due to the increasing receiving power by a pair of PV panels, when the intercept ratio reaches up to 0.52. Above results tell that TFFC obtains distinct advantage than traditional PTC systems. The improvements depend on specific design parameters including reflector aperture size, PV concentration, PV ratio, etc…

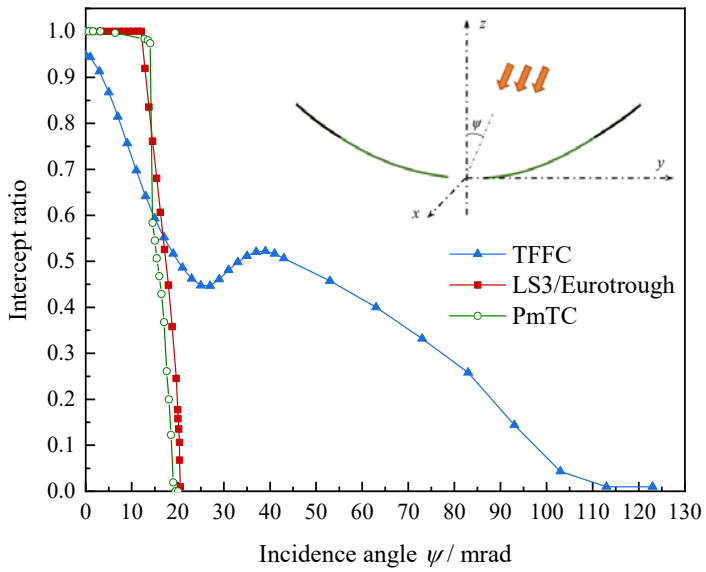

Figure 12. Angle transmission curve comparison.

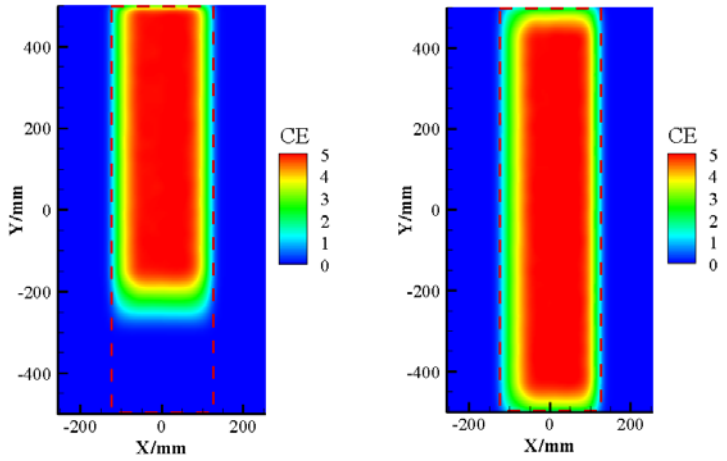

(a) Rotation 3° in y-axis (b) Rotation 3° in x-axis

Figure 13. The 2-D heat flux distributions with different tracking angles.

Most of the trough solar concentrating system adopts 2-D tracking manner which placed the concentrators along north-south axis simultaneously tracking the sun from east to west throughout the day. This makes the concentrating solar rays skew along y-axis when tracking the sun, as Figure 13(a) shows. It can be seen that the receiving sunlight has been transferred to $y > 0$ side for about 200 mm when the rotation angle in y-axis is set as 3°. Compared with the result of ideal condition in Figure 8(b), the remaining heat flux distribution on cross section of the receiver changes slightly. For PVR modules, the changing of heat flux intensity at tracking status must be considered when arranging the series parallel circuit and optimize the I-V characteristics.

The tracking error in x-axis, on the other hand, has a small influence on heat flux distribution, as can be seen in Figure 13(b). For the case of rotation 3° in x-axis, the main distribution had been slightly transferred along y-axis. Therefore, the utilization of TFFC can largely reduce the tolerance limit of the tracking error that makes it more practical.

Compared with thermal power, electricity is treated as a kind of high-grade power based on the second law of thermodynamics, although they are equal according to first law of thermodynamics. Coventry [29] studied different methods for finding an electrical to thermal ratio for the useful energy conversion in a PVT system. An energy definition is given as follows:

$$E_{\mathrm{Eq,Elec}} = \frac{E_{\mathrm{Th}}}{[\text{Energy value ratio}]} + E_{\mathrm{Elec}}$$

Above ratio is called equivalent electrical energy (Coventry and Lovegrove, 2001), which is an comprehensible evaluation index for the calculation of minimum possible 'equivalent electrical levelized energy cost'. Assume that the energy value ratio is equal to 5.0, length along x-axis for concentrator is 10 m, the equivalent electrical energy for PTC with 35 mm and 58 mm tube and TFFC with PV efficiency of 0.18 and 0.25 can be solved as Figure 14 shows.

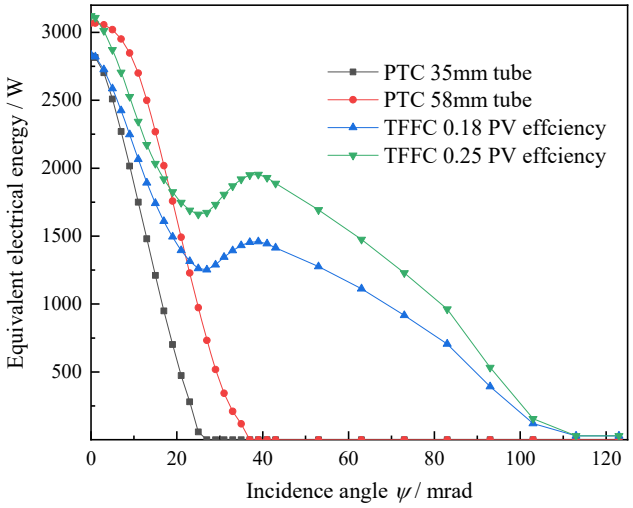

Figure 14. Equivalent electrical energy at different incidence angle rotated in x-axis.

We can find that traditional PTC using 58 mm thermal tube obtains advantage at low incidence angle below 40 mrad. PTC using 35 mm tube receives the lowest equivalent electrical energy because of obvious optical loss. On the other hand, the equivalent electrical energy of new designed TFFC becomes higher after around 30 mrad incidence and peaks at 40 mrad. The changing trend is similar with intercept ratio results in Figure 14. PV efficiency is a main factor that decides the equivalent energy value. TFFC with 0.25 PV efficiency will has much higher energy production than the one in 0.18 PV efficiency. The absolute value also depends on the energy value ratio that will not be discussed here. In general, new designed TFFC proposed by the current study has apparent advantage at high incidence angle which is rather important for the consideration of aging phenomenon of solar tracking system and reflecting mirrors. The proposed system is suitable for solar power station with the demand of combined thermal and electricity generation. The results provide a reference for novel free-form solar energy applications, which we plan to manufacture and test experimentally in the near future.

5. Conclusions

The current study aims to achieve higher optical efficiency for PTC by extending the aperture size using freeform optics and combined PV/thermal utilization. With the aid of geometric construction modelling and ray tracing method, the optical characteristic has been investigated to verify the effective modelling. The following conclusions are drawn:

(1) Sensitivity analysis results tells that TFFC is suitable for large aperture size and error factor. The concentrated heat flux remains high uniformity and coincides with the preset CG.

(2) The energy allocation for PV/Thermal use makes great impact on optical performance of TFFC. A reasonable CG is necessary in practical application when low a PV ratio was selected.

(3) The effect of tracking errors has been investigated. The utilization of TFFC can largely reduce the tolerance limit of the tracking error that makes it more practical. This is an inspiring result for the control of optical loss when we replace a part of freeform surface to the original PTC.

(4) Considering the effect of equivalent total power, new designed TFFC has apparent advantage at high incidence angle which is rather important for the consideration of aging phenomenon of solar tracking system and reflecting mirrors.

The above results are promising and significant for the enhancement of trough type solar concentrator systems.

Acknowledgements

This work was financially support through National Natural Science Foundation of China (No. 51806180), China Postdoctoral Science Foundation (No. 2018M641018) and Shaanxi Province Postdoctoral Science Foundation (No. 2018BSHTDZZ09).

Conflict of interest

We declare that we have no financial and personal relationships with other people or organizations that can inappropriately influence our work, there is no professional or other personal interest of any nature or kind in any product, service and/or company that could be construed as influencing the position presented in, or the review of, the manuscript entitled.

Appendix

The discrete points of freeform surface for the case of Table 1 are as follows (in millimeter):

Point number	Y coordinate	Z coordinate	Point number	Y coordinate	Z coordinate
1	2930.0	910.1	26	3526.9	1302.1
2	2953.9	924.6	27	3550.8	1319.0
3	2977.8	939.3	28	3574.7	1336.0
4	3001.6	954.0	29	3598.6	1353.1
5	3025.5	968.8	30	3622.4	1370.3
6	3049.4	983.7	31	3646.3	1387.6
7	3073.3	998.7	32	3670.2	1405.0
8	3097.1	1013.9	33	3694.1	1422.4
9	3121.0	1029.1	34	3718.0	1440.0
10	3144.9	1044.4	35	3741.8	1457.6
11	3168.8	1059.8	36	3765.7	1475.4
12	3192.7	1075.3	37	3789.6	1493.2
13	3216.5	1090.9	38	3813.5	1511.2
14	3240.4	1106.5	39	3837.3	1529.2
15	3264.3	1122.3	40	3861.2	1547.3
16	3288.2	1138.2	41	3885.1	1565.5
17	3312.0	1154.2	42	3909.0	1583.8
18	3335.9	1170.2	43	3932.9	1602.2
19	3359.8	1186.4	44	3956.7	1620.7
20	3383.7	1202.6	45	3980.6	1639.3
21	3407.6	1219.0	46	4004.5	1657.9
22	3431.4	1235.4	47	4028.4	1676.7
23	3455.3	1251.9	48	4052.2	1695.6
24	3479.2	1268.6	49	4076.1	1714.5
25	3503.1	1285.3	50	4100.0	1733.5

References

1. Islam MT, Huda N, Abdullah AB, et al. (2018) A comprehensive review of state-of-the-art concentrating solar power (CSP) technologies: Current status and research trends. *Renewable Sustainable Energy Rev* 91: 987–1018.
2. Wang Q, Hu M, Yang H, et al. (2019) Energetic and exergetic analyses on structural optimized parabolic trough solar receivers in a concentrated solar–thermal collector system. *Energy* 171: 611–623.
3. Wang Q, Yang H, Zhong S, et al. (2020) Comprehensive experimental testing and analysis on parabolic trough solar receiver integrated with radiation shield. *Appl Energy* 268: 115004.
4. Wang F, Cheng Z, Tan J, et al. (2017) Progress in concentrated solar power technology with parabolic trough collector system: A comprehensive review. *Renewable Sustainable Energy Rev* 79: 1314–1328.

5. Núnez Bootello JP, Schramm M, Silva AS, et al. (2017) Parametric trough solar collector with commercial evacuated receiver: Performance comparison at plant level. *J Sol Energy Eng* 139: 041014.
6. Bootello JPN, Price H, Perez MS, et al. (2016) Optical analysis of a two stage XX concentrator for parametric trough primary and tubular absorber with application in solar thermal energy trough power plants. *J Sol Energy Eng* 138: 041002-1.
7. Miñano JC, Benítez P, Santamaría A (2009) Free-form optics for illumination. *Opt Rev* 16: 99–102.
8. Luo Y, Feng Z, Han Y, et al. (2010) Design of compact and smooth free-form optical system with uniform illuminance for LED source. *Opt Express* 18: 9055–9063.
9. Reimers J, Schiesser EM, Thompson K, et al. (2015) Comparison of freeform imaging spectrometer design forms using spectral full-field displays. *Freeform Opt*, FM3B. 3.
10. Fournier F, Rolland J (2008) Optimization of freeform lightpipes for light-emitting-diode projectors. *Appl Opt* 47: 957–966.
11. Hernández M, Benítez P, Miñano J, et al. (2007) The XR nonimaging photovoltaic concentrator. *Proceedings of SPIE, Nonimaging Optics and Efficient Illumination Systems IV*, 667005–667010.
12. Cui SF, Nicholas P, Liliana RD, et al. (2019) Silicone optical elements for cost-effective freeform solar concentration. *Opt Express* 27: A572–A580.
13. Cvetkovic A, Hernandez M, Benítez P, et al. (2008) The free form XR photovoltaic concentrator: a high performance SMS3D design. *Proceedings of SPIE—The International Society for Optical Engineering*: 7043.
14. Hernández M, Benítez P, Miñano J, et al. (2007) XR: A high-performance PV concentrator. *Proceedings of SPIE*, 664904–664910.
15. Cvetkovića A, Hernandezb M, Beníteza P, et al. (2008) The SMS3D photovoltaic concentrator. *Proceedings of SPIE—The International Society for Optical Engineering* 7059: 705909.1–705909.12.
16. Miñano J, Hernandez M, Benítez P, et al. (2005) Free-form integrator array optics. *Proceedings of the SPIE*: 114–125.
17. Symko-Davies M (2007) High and low concentration for solar electric applications ii. *Proceedings of SPIE—The International Society for Optical Engineering*, 6339.
18. Zamora P, Cvetkovic A, Buljan M, et al. (2009) Advanced PV concentrators. *Photovoltaic Specialists Conference (PVSC)* 34th IEEE: 000929–000932.
19. Benítez P, Miñano JC, Zamora P, et al. (2010) High performance Fresnel-based photovoltaic concentrator. *Opt Express* 18: A25–A40.
20. Miñano JC, Benítez P, Zamora P, et al. (2013) Free-form optics for Fresnel-lens-based photovoltaic concentrators. *Opt Express* 21: A494–A502.
21. Alvarez JL, Hernandez M, Benitez P, et al. (2001) TIR-R concentrator: a new compact high-gain SMS design. *Proc. SPIE 4446, Nonimaging Optics: Maximum Efficiency Light Transfer VI*.
22. Benítez P, Miñano JC (2007) The Future of illumination design. *Opt Photonics News* 18: 20–25.
23. Cheng D, Wang Y, Hua H (2010) Free form optical system design with differential equations. *International Society for Optics and Photonics*, 78490Q-78490Q-78498.
24. Ries H, Muschaweck J (2002) Tailored freeform optical surfaces. JOSA A 19: 590–595.
25. Fournier FR, Cassarly WJ, Rolland JP (2010) Fast freeform reflector generation using source-target maps. *Opt Express* 18: 5295–5304.

26. Dross O, Mohedano R, Benitez P, et al. (2004) Review of SMS design methods and real-world applications. *Proceedings of SPIE—The International Society for Optical Engineering* 5529: 35–47.
27. Tsai CY (2015) Improved irradiance distribution on high concentration solar cell using free-form concentrator. *Sol Energy* 115: 694–707.
28. Cheng Y, Fang F, Zhang X (2012) Design and manufacture of off-axis optical reflective integrator with faceted structure. *Opt Eng* 51: 4001.
29. Coventry JS, Lovegrove K (2003) Development of an approach to compare the 'value' of electrical and thermal output from a domestic pv/thermal system. *Sol Energy* 75: 63–72.

AIMS Press